

Influence of SMAs on the attenuation of effects of P- Δ type in shear frames

Ottavia Corbi†

University of Naples "Federico II", Dept. "Scienza delle Costruzioni", via Claudio 21,
80125, Naples, Italy

(Received June 2, 2003, Accepted December 18, 2003)

Abstract. In the paper one investigates the benefits deriving from the introduction of SMA provisions in a structure subject to dynamic excitation and vertical loads. At this purpose one considers a multi-degree-of-freedom (mdof) shear elastic-plastic frame and designs couples of super-elastic SMA tendons to be placed at critical locations of the structure. Particular attention is focused on the reduction of P- Δ effects.

Key words: structural dynamics; smart materials; semi-active devices; shape memory alloys.

1. Introduction

Advances in structural control have given rise to the new concept of structures acting like dynamic systems, which are suitably equipped with devices in such a way to somehow interact with the incoming excitation.

Recently a significant effort has been devoted to the design of control schemes based on *intelligent materials*. The basic idea is to build new classes of sensors and actuators taking advantages of *special behaviours* such as those of piezoelectric, electrorheologic and magnetorheologic materials or shape memory alloys.

A class of devices, which is particularly interesting as regards the suppression of dynamic vibrations in engineering structures, is related to the application of "smart materials". Generally speaking, new technologies linked to the adoption of such materials are very promising because of their mechanical simplicity, low energy demand, skill of generating high intensity forces and, definitively, robustness.

Particularly attractive for civil engineering applications are the Shape Memory Alloys (SMAs), which are characterized by special properties, due to micro-crystalline phase transition processes (Duerig *et al.* 1992, Liu and Van Humbeeck 1999, Srinivasan and McFarland 2000).

SMAs exhibit a complex load-deformation-temperature behaviour (Buehler and Wiley 1965, Funakubo 1984, Muller 1992, Wayman 1990, 1992), which is characterized by hysteresis loops in the stress-strain diagrams (it is usually termed "quasi-plastic" at low temperature and "pseudo-elastic" at high temperature), and in the deformation-temperature diagram.

†Assistant Professor in Structural Mechanics

This capacity results in two major features at the macroscopic level: shape memory effect (depending on the capability in recovering possible accumulated deformations by heat treatment) and super-elasticity (i.e. the recovery of large deformations in loading-unloading cycles, occurring at sufficiently high temperatures).

Actually, research on SMA applications in civil engineering have concentrated along two main directions, i.e., on one side, the use of shape memory effect for developing actuators for active control of system dynamics, and, on the other side, (Baz *et al.* 1990, Ikegami *et al.* 1990, MacLean *et al.* 1991), the exploitation of high damping resulting from pseudo-elasticity to passive vibration control (Baratta and Corbi 2003, Corbi 2001, Dolce *et al.* 2000, Liang and Rogers 1993, Liu and Van Humbeeck 1999, Thomson *et al.* 1995).

The SMAs super-elasticity, under dynamic loading, gives rise to inelastic deformation, producing damping and centring effects, which are pretty desirable for applications in the field of earthquake resistant engineering.

Under this perspective, the paper aims at pointing out the benefits that the SMA super-elastic behaviour can introduce in the dynamical response of a mdof structural model, with special reference to the case when dynamical loads interact with P- Δ effects. This purpose is pursued by designing a reinforcement system consisting of SMA pseudo-elastic tendons to be introduced at the levels that mostly suffer the dynamic excitation.

2. The 7-dof plastic frame

2.1. The reference model

Let consider the structural model depicted in Fig. 1(a), which represents a 7-dof shear-type frame; the model is assumed to exhibit an elastic-perfectly-plastic behaviour and its characteristics, in terms of i -th storey mass m_i , stiffness k_i , damping c_i , yield displacements u'_{oi} , u''_{oi} and shear T'_{oi} , T''_{oi} limits (positive in the rightward direction and negative in the leftward direction) are given in Table 1.

In the following paragraph details are given concerning the simulation of the dynamic response of such structure under the action of a base acceleration.

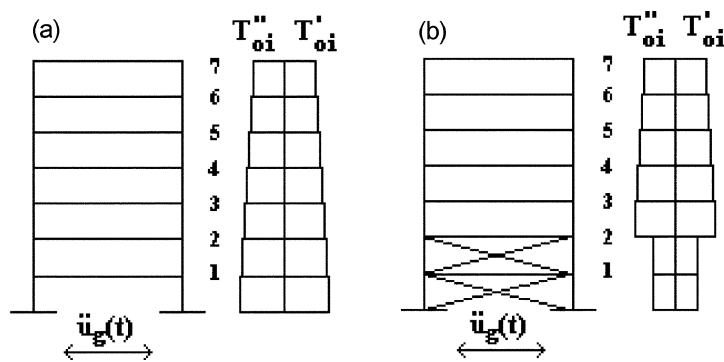


Fig. 1 7-dof shear frame: (a) without SMA tendons; (b) with SMA tendons

Table 1. Simple shear frame

i^{th} floor	m_i (kg · sec ² /cm)	c_i (kg · sec/cm)	k_i (kg/cm)	u'_{oi}, u''_{oi} (cm)	T'_{oi}, T''_{oi} (kg)
1	20	200.000	200000	±0.056898	±11379.6
2	16	185.714	185714	±0.058357	±10837.71
3	16	171.439	171439	±0.060059	±10295.83
4	16	157.142	157142	±0.062070	±9753.943
5	16	142.857	142857	±0.064484	±9212.058
6	16	128.571	128571	±0.067435	±8670.172
7	16	114.286	114286	±0.071122	±8128.286

2.2. Mathematical formulation and numerical implementation

The dynamic analysis of the elastic-perfectly plastic n -storey shear frame is performed step by step by implementing (in ad-hoc compiled code) the basic dynamic equilibrium equations. A short synthesis of the overall mathematical and numerical approach is given in the following.

After discretizing the total time of simulation T_{len} ($\geq T_{fin}$, i.e. the duration of the forcing function) in a number of intervals with time-length Δt such that the relation $t^{(r)} = r \cdot \Delta t$ holds for the single sample time $t^{(r)}$, consequently one operates the discretization of the time response variables, which are denoted by the apex $(\cdot)^{(r)}$ at time $t^{(r)}$.

With reference to the i -th floor, which is denoted by the pedex $(\cdot)_i$, one introduces the expressions of storey displacements $u_i^{(r)}$, velocities $\dot{u}_i^{(r)}$ and accelerations $\ddot{u}_i^{(r)}$ at time $t^{(r)}$, and, thereafter, those of inter-storey drifts (splitted into the elastic and plastic components), velocities and accelerations

$$\begin{aligned} \Delta_{ui}^{(r)} &= u_i^{(r)} - u_{i-1}^{(r)}, \quad \Delta_{\dot{u}i}^{(r)} = \dot{u}_i^{(r)} - \dot{u}_{i-1}^{(r)}, \quad \Delta_{\ddot{u}i}^{(r)} = \ddot{u}_i^{(r)} - \ddot{u}_{i-1}^{(r)} \\ \Delta_{ui}^{(r)} &= \Delta_{eli}^{(r)} + \Delta_{pli}^{(r)} \rightarrow \Delta_{eli}^{(r)} = \Delta_{ui}^{(r)} - \Delta_{pli}^{(r)} \end{aligned} \quad (1)$$

In the inter-storey displacement one can recognise an elastic $\Delta_{eli}^{(r)}$ and a plastic $\Delta_{pli}^{(r)}$ component contributing to the total drift. Splitting the storey force $T_i^{(r)}$ in the two components related to the elastic displacement and to the velocity

$$\begin{aligned} T_i^{(r)} &= T_{ui}^{(r)} + T_{\dot{u}i}^{(r)} \\ T_{ui}^{(r)} &= k_i \Delta_{eli}^{(r)}, \quad T_{\dot{u}i}^{(r)} = c_i \Delta_{\dot{u}i}^{(r)} \end{aligned} \quad (2)$$

one can evaluate the two reactive force components contributing to the dynamic equilibrium of the i -th floor

$$\begin{aligned} R_i^{(r)} &= R_{ui}^{(r)} + R_{\dot{u}i}^{(r)} = T_i^{(r)} - T_{i+1}^{(r)} \\ R_{ui}^{(r)} &= T_{ui}^{(r)} - T_{ui+1}^{(r)}, \quad R_{\dot{u}i}^{(r)} = T_{\dot{u}i}^{(r)} - T_{\dot{u}i+1}^{(r)} \end{aligned} \quad (3)$$

The dynamic equilibrium equation can, thus, be written, at the i -th floor, in the form

$$\ddot{u}_i^{(r)} = -\frac{1}{m_i}(m_i\ddot{u}_g^{(r)} + R_i^{(r)}) \quad (4)$$

with $\ddot{u}_g^{(r)}$ the instantaneous value (at time $t^{(r)}$) of the ground acceleration.

If some vertical loads w_i are considered (for example related to the weight of the upper floors, calculated through the backward recursive formula $w_i = w_{i+1} + m_i g$, with g the gravity acceleration and $w_n = m_n g$), P- Δ effects should also be accounted for by adding in the parenthesis at the right side of Eq. (4) the term related to such loads.

In this case Eq. (4) turns into

$$\ddot{u}_i^{(r)} = -\frac{1}{m_i}\left(m_i\ddot{u}_g^{(r)} + R_i^{(r)} - \frac{w_i\Delta_{ui}^{(r)}}{h_i} + \frac{w_{i+1}\Delta_{ui+1}^{(r)}}{h_{i+1}}\right) \quad (5)$$

where h_i denotes the height of the i -th floor.

Starting from the initial rest condition (when all of the response variables are zero) one can assume a step rationale of the type

$$\begin{aligned} u_i^{(r+1)} &= u_i^{(r)} + \dot{u}_i^{(r)} \cdot \Delta t + \ddot{u}_i^{(r)} \cdot \frac{\Delta t^2}{2} \\ \dot{u}_i^{(r+1)} &= \dot{u}_i^{(r)} + \ddot{u}_i^{(r)} \cdot \Delta t \end{aligned} \quad (6)$$

where $\ddot{u}_i^{(r)}$ is given (for $i = 1 \dots n$) by Eq. (4) or Eq. (5) depending on if P- Δ effects are considered or not. Eqs. (6) gives the updating relations for the storey displacement and velocity variables.

Obviously at each time step it is necessary to check if some plastic excursions have occurred, by introducing some suitably defined tests for the two loading directions, i.e.

Test 1 Plastic excursions

If $[\Delta_{ui}^{(r+1)} - \Delta_{pli}^{(r+1)} > \Delta_{oi}']$ and $[\Delta_{ui}^{(r+1)} > 0]$	\rightarrow	Rightward excursion $I_{pl} = +1$
If $[\Delta_{ui}^{(r+1)} - \Delta_{pli}^{(r+1)} < \Delta_{oi}'']$ and $[\Delta_{ui}^{(r+1)} < 0]$	\rightarrow	Leftward excursion $I_{pl} = -1$

being Δ_{oi}' , Δ_{oi}'' the yield limits of the floor drift in the rightward and in the leftward direction respectively

$$\Delta_{oi}' = \frac{T_{oi}'}{k_i} > 0; \quad \Delta_{oi}'' = \frac{T_{oi}''}{k_i} < 0$$

and $T_{oi}' > 0$, $T_{oi}'' < 0$ the limit rightward and leftward shear forces.

If one of the two conditions is satisfied, the floor is experimenting a plastic excursion (in the positive or negative direction depending on the sign of the index I_{pl}), for which the updating of the plastic drift is also required

$$\Delta_{pli}^{(r+1)} = \Delta_{pli}^{(r)} + \Delta_{ui}^{(r)} \cdot \Delta t + \Delta_{ui}^{(r)} \cdot \frac{\Delta t^2}{2} \quad (7)$$

Some tests relevant to possible coming back from the plastic phase into the elastic phase should be introduced as well, i.e.

Test 2 Elastic re-entries

If $[\Delta_{ai}^{(r+1)} < 0]$ and $I_{pl} = +1$	→	Rightward re-entry → $I_{pl}=0$
If $[\Delta_{ai}^{(r+1)} > 0]$ and $I_{pl} = -1$	→	Leftward re-entry → $I_{pl}=0$

Thereafter one can update the acceleration expression iterating the whole procedure until the final T_{len} is reached.

The last remark is that in order to achieve accurate results in the calculation, some adjustments on the time interval Δt are required, which must be locally re-tuned (i.e. suitably reduced) in order to fit the instant of crossing of the plastic threshold (from above or below) with calibrated accuracy. The result is that Δt remains uniform on the whole t-axis, with the exception of the intervals including instants where plastic excursion starts and/or elastic recovery occurs.

2.3. Numerical testing

For numerical testing the considered n -dof structural model is assumed to be subject to a ground acceleration expressed by a sine wave modulated function (Fig. 2) with duration $T_{fin} = 4$ secs, of the type $\ddot{u}_g(t) = \ddot{u}_{go} \cdot \sin(\omega_g t) \cdot t \cdot e^{-\lambda t}$ with t the time variable, $\ddot{u}_{go} = 1275.30 \text{ cm} \cdot \text{sec}^{-2}$, $\omega_g = 20 \text{ sec}^{-1}$ and $\lambda = 5/T_{fin}$. The maximum absolute value attained by the ground acceleration is equal to $\max_{t \in [0, T_{fin}]} |\ddot{u}_g(t)| = 562.89 \text{ cm} \cdot \text{sec}^{-2}$.

By means of the code whose implementation has been described in the previous Sect. 2.2, the structural system is kept under observation for a time interval $T_{len} = 6$ secs. One also considers the case when vertical loads related to the structure self-weight are applied, thus introducing P-Δ effects.

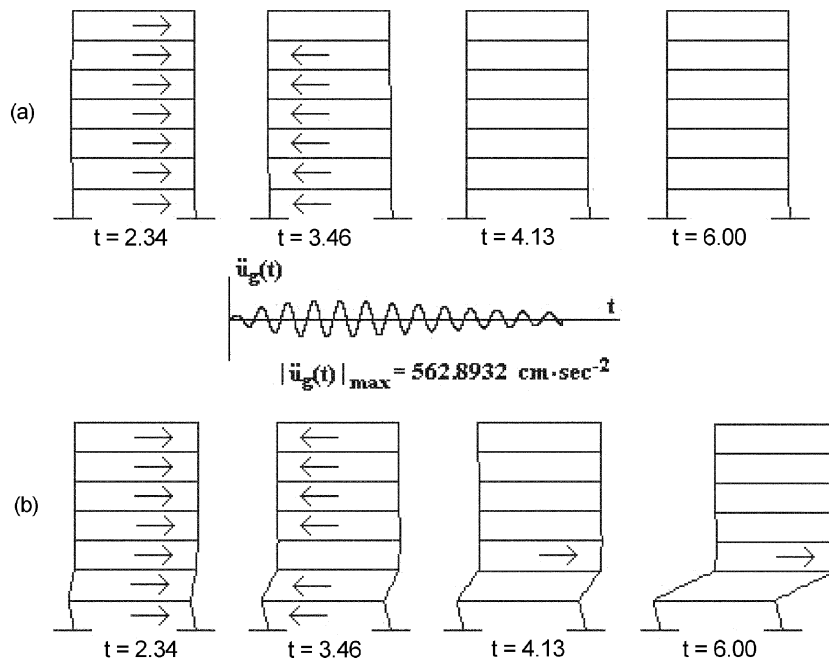


Fig. 2 Sketches of the shear frame during the motion: (a) without P-Δ effect, (b) with P-Δ effect

In Fig. 2 one reports some sketches of the shear frame motion under the given forcing function for the two cases (Fig. 2(a), shear frame without $P-\Delta$ effects and Fig. 2(b), shear frame with $P-\Delta$ effects) at different time instants: arrows indicate the directions of plastic excursions when they occur.

As one can observe ordinary plastic deformations occur at each floor of the structure during the motion under simply horizontal dynamic loads (Fig. 2(a)), while, when adding vertical loads (Fig. 2(b)), wide plastic excursions occur at first and second floor and quickly lead the structure to the failure, which is attained at the second floor.

3. The 7-dof plastic frame equipped with SMA provisions

3.1. The reference model equipped with SMA provisions

In order to prevent the structure from the development of too large hysteresis loops that may cause its collapse, one considers the possibility of exploiting the super-elasticity of SMAs, by introducing SMA members at the most solicited floors in such a way to dissipate most of the incoming dynamic energy.

The objective of such an approach is to provide the main structure with dissipation devices (located at “weak points”) able to attenuate the effects induced by the incoming dynamic excitation also in terms of recovering of residual plastic deformations; obviously, the exploitation of the pseudo-elastic character of the SMA members requires a suitable tuning of the alloy parameters on the basis of the structure mechanical and geometrical characteristics.

In the specific case, one designs (Corbi 2001, Baratta and Corbi 2003) two couples of SMA tendons to be introduced in the lower part of the structure, at the first and second floor (Fig. 1(b)), which represent the most solicited storeys (as clear from Fig. 2). The design of the SMA elements is tuned on the structure characteristics in such a manner to make the SMA elements exhibit hysteresis loops, i.e. the classical super-elastic behaviour.

Details about the design stage and its implementation in a computer code are provided in Sect. 3.3, after discussing the choice of the adopted constitutive model in the following Sect. 3.2.

3.2. Considerations about constitutive SMA models

For suitably designing dissipative SMA members, one should emphasize that much attention is to be paid to the proper choice of the alloy constitutive model. Actually, as a consequence of the increasing scientific and commercial interest attracted by SMAs, many constitutive models, operating at the microscopic and macroscopic level, able to reproduce more or less roughly the main characters of their behaviour have been proposed in literature; the choice of the model, thus, need some discussion.

The behaviour of SMA elements, as well known, is somewhat dependent on thermo-mechanical coupling; a number of pretty complex models taking into account this effect do exist, as discussed by Graesser and Cozzarelli (1994) and Maclean (1989). Actually the high sophistication of these models make them pretty unsuitable for practical investigations concerning possible engineering applications and pushes towards the adoption of simplified models able to capture the essential features of the alloy mechanical behaviour.

In the paper, for representing the pseudo-elastic (or super-elastic) SMA behaviour, one refers to a one-dimensional isothermal SMA constitutive relation (Armstrong 1996, Baratta and Corbi 2003, Corbi 2001, Graessel and Cozzarelli 1991, 1994, Feng and Li 1996), substantially developed as an

extension of the Bouc-Wen hysteretic model (Wen 1976) on the basis of experimental studies and deduced by a general material characterization.

The choice of such a model is based on some fundamental considerations that allow to neglect, at a first stage, thermo-mechanical coupling.

In practice, SMA materials exhibit hysteresis cycles with a dissipated energy amount that, substantially, does not depend on temperature. This effect is demonstrated by experimental evidence that shows that the threshold for forward (A→M) transformations (and for triggering the apparent plastic phase) rises at a rate of the order $5 \div 7$ MPa per °C, only dragging upward the whole hysteresis loop, which remains unvaried in its amplitude.

The material temperature changes during the deformation, due to the latent transformation heat and to the dissipation of energy during the cycle. Considering that the temperature decreases during the reverse transformation, the overall result is a kind of apparent kinematic strain hardening, which may be significant when the strain velocity is large.

Therefore, when neglecting the temperature variation during deformation, one adopts a degree of approximation that is comparable to assuming the perfectly plastic behaviour in elastic-plastic analyses, where strain hardening is often ignored.

One might add that some experimental evidence (Dolce *et al.* 2000) would prove that temperature effects are mitigated when the size of the SMA elements increases: so it is more significant for wires than for gross bars. Anyway, a lot of research in theoretical, experimental and numerical simulation of structural response under earthquake-type disturbances allows to conclude that strain-hardening invariably produces an improvement in the structure seismic performance; therefore the adopted simplified approach for the SMA case is expected to produce results advantaging structural safety.

Finally, the importance of thermal coupling in seismic response of structures endowed with SMA components has not yet been definitely assessed.

In synthesis, one can conclude that neglecting the thermo-mechanical coupling does not affect so much the essence of the SMA contribution to the structural response.

On the other side, the paper aims at exploiting the chances offered by the super-elasticity properties of the shape-memory-alloys, quite apart from other effects; the simplification of the model (which is detailed in the following Sect. 3.3) is practically mandatory at this stage of the research, in order to have neatly intelligible results not marred by secondary side phenomena.

3.3. Mathematical formulation and numerical implementation

If some SMA tendons are introduced in the structure at defined locations, further actions contributing to the dynamic equilibrium of the structure should be considered.

The presence of SMA tendons (which are assumed to be unilateral, i.e. to be unable to sustain compression, thus being alternatively activated depending on which one is currently subject to tensile stress) requires the introduction of additive terms in the dynamic equations relevant to each floor. For each floor, say the i -th one, one defines two possible *positive* tendons, both directed up-rightwards when looking at the floors from the ground to the top: one with the *origin* at the left extrados of the i -th floor characterised at time $t^{(r)}$ by normal force $N_{io}^{+(r)}$ and the second with the *end* at the right intrados of the same floor, characterised at time $t^{(r)}$ by normal force $N_{ie}^{+(r)}$. Analogously, one defines two possible *negative* tendons for the generic i -th floor, both directed up-leftwards: one with the *origin* at the right extrados of the i -th floor characterised at time $t^{(r)}$ by normal force $N_{io}^{-(r)}$ and the second with the *end* at the left intrados of the same floor, characterised at time $t^{(r)}$ by normal

force $N_{ie}^{-(r)}$. Note that normal forces of tendons having the origin on the i -th floor are denoted by the suffix “o”, while normal forces of tendons having the extremity on the same floor are identified by the suffix “e”. Similar notations hold for the angles $\alpha_{io}^{+(r)}$, $\alpha_{ie}^{+(r)}$, $\alpha_{io}^{-(r)}$, $\alpha_{ie}^{-(r)}$ that the tendons instantaneously form with the floor.

Therefore, the equations of dynamic equilibrium at floors where tendons contribution are to be considered turn into

$$\ddot{u}_i^{(r)} = -\frac{1}{m_i}(m_i\ddot{u}_g^{(r)} + R_i^{(r)}) + \frac{N_{io}^{+(r)} \cos \alpha_{io}^{+(r)} - N_{ie}^{+(r)} \cos \alpha_{ie}^{+(r)} - N_{io}^{-(r)} \cos \alpha_{io}^{-(r)} + N_{ie}^{-(r)} \cos \alpha_{ie}^{-(r)}}{m_i} \quad (8)$$

being intended that the normal forces in the tendons are null if the relevant strain is negative (i.e. if the tendon is in a shortening phase).

If P- Δ effects are considered, one can re-write the equilibrium conditions Eq. (8) as follows

$$\begin{aligned} \ddot{u}_i^{(r)} = & -\frac{1}{m_i} \left(m_i \ddot{u}_g^{(r)} + R_i^{(r)} - \frac{w_i \Delta_{ui}^{(r)}}{h_i} + \frac{w_{i+1} \Delta_{ui+1}^{(r)}}{h_{i+1}} \right) + \\ & + \frac{N_{io}^{+(r)} \cos \alpha_{io}^{+(r)} - N_{ie}^{+(r)} \cos \alpha_{ie}^{+(r)} - N_{io}^{-(r)} \cos \alpha_{io}^{-(r)} + N_{ie}^{-(r)} \cos \alpha_{ie}^{-(r)}}{m_i} \end{aligned} \quad (9)$$

In the specific case, with reference to the considered 7-dof shear frame, two couples of tendons are introduced at the first two levels; therefore one has to instantaneously determine the forces $N_{ie}^{+(r)}$, $N_{ie}^{-(r)}$, $N_{lo}^{+(r)} = N_{2e}^{+(r)}$, $N_{lo}^{-(r)} = N_{2e}^{-(r)}$ exerted by the stretched SMA tendons (actually $N_{ie}^{+(r)}$ if $N_{ie}^{+(r)} > 0$, or $N_{ie}^{-(r)}$ if $N_{ie}^{-(r)} > 0$; and $N_{lo}^{+(r)} = N_{2e}^{+(r)}$ if $N_{lo}^{+(r)} > 0$ or $N_{lo}^{-(r)} = N_{2e}^{-(r)}$ if $N_{lo}^{-(r)} > 0$).

This objective can be accomplished once the basic SMA stress-strain relations are assumed; thus, it requires a quite consistent preliminary work (mainly finalised to the suitable tuning of the SMA parameters), which consists of a number of steps that are shown in the following.

3.3.1. Step 1: selecting the SMA mechanical model

At this purpose, in order to focus the attention on the pseudo-elastic feature of these alloys, one refers to the above-cited isothermal uni-axial model (Graesser and Cozzarelli 1994), which has been modified (Corbi 2001) for reducing the computational effort and especially for solving some modelling problems.

In details, the SMA material characterisation can be performed by means of an extension of a rate-independent hysteretic model proposed by Ozdemir (1976). The Ozdemir’s model, which has been shown (Constantinou and Adnane 1987) to represent a special case of the Bouc-Wen model (Wen 1976), gives the uni-axial rate relation σ - ε , according to

$$\begin{cases} \dot{\sigma} = E \left[\dot{\varepsilon} - \left| \dot{\varepsilon} \left(\frac{\sigma - \beta}{\sigma_c} \right)^d \right| \right], & \dot{\varepsilon} = \frac{\dot{\sigma}}{E} + \left| \dot{\varepsilon} \left(\frac{\sigma - \beta}{\sigma_c} \right)^d \right| = \frac{\dot{\sigma}}{E} + \varepsilon_{in} \\ \dot{\beta} = E \gamma \left| \dot{\varepsilon} \left[\frac{\sigma - \beta}{\sigma_c} \right]^d \right| \end{cases} \quad (10)$$

In Eq. (10) the back-stress β plays the role of the internal variable, the deformation is given by superposition of an elastic component and of an inelastic component ε_{in} linked to the difference $\sigma - \beta$ (which represents the over-stress), the parameter d controls the accuracy of the transition from the pre-yielding

to the post-yielding phase, the Young modulus E determines the slope of the curve in the pre-yielding region, the critical stress σ_c is equal to one-half the amplitude of the hysteretic cycle, whilst the parameter γ is, somehow, related to both the slope of the inelastic curve and the cycle amplitude.

In order to account for the SMA behaviour, some changes have been proposed (Graesser and Cozzarelli 1991, 1994) to the Ozdemir's model, yielding the relations

$$\left\{ \begin{array}{l} \dot{\sigma} = E \left[\dot{\varepsilon} - |\dot{\varepsilon}| \left| \frac{\sigma - \beta}{\sigma_c} \right|^{d-1} \left(\frac{\sigma - \beta}{\sigma_c} \right) \right] \\ \beta = E\gamma \left[\left(\hat{\varepsilon} - \frac{\sigma}{E} \right) + \psi |\varepsilon|^p \operatorname{erf}(\xi \varepsilon) \right] = E\gamma [\varepsilon_{in} + \psi |\varepsilon|^p \operatorname{erf}(\xi \varepsilon)] \end{array} \right. \quad \text{with } \left\{ \operatorname{erf}(x) = \frac{2}{\sqrt{\pi}} \int_0^x 2^{-t^2} dt \right. \quad (11)$$

where the error function $\operatorname{erf}(\cdot)$ has the effect of causing the inelastic strain to decrease upon unloading (the inelastic strain can be, thus, fully recovered upon complete unloading), whilst the other material parameters should be suitably tuned in order to make the SMA to exhibit the classical pseudo-elastic behaviour.

Actually a careful analysis of the model given in Eq. (11) shows that some problems may arise due to modelling errors and to the computational feature (Feng and Li 1996):

- i) for $\varepsilon \ll 1$ the curve σ - ε is not exactly linear, as one can observe from Fig. 3, which has been obtained by numerically implementing the model under imposed deformation cycles;
- ii) for $\sigma \rightarrow 0$ after a loading cycle, a residual deformation can be noticed (which means that, close to the origin, the diagram σ - ε is plaited; this effect is a pretty undesirable feature since it is associated to a negative hysteresis upon unloading causing abnormal energy production);
- iii) The numerical implementation of the model is computationally heavy.

In order to solve all of these problems, in previous papers a variant of the model (Baratta and Corbi 2003, Corbi 2001) has been proposed, able to completely suppress the modelling error in the unloading and to consistently lighten the numerical implementation of the model.

The changes introduced in the original model by Graesser and Cozzarelli Eq. (11) are

$$\gamma = \frac{\sigma_o - \sigma_c}{E\psi - \sigma_o}, \quad \psi = c_\psi \frac{\sigma_c}{E}, \quad \sigma_c = \nu \sigma_o$$

$$\operatorname{erf}(x) \Leftrightarrow \frac{2}{\pi} \arctan(\bar{x}), \quad \bar{x} = x^3 |x|^q, \quad q < 1 \quad (12)$$

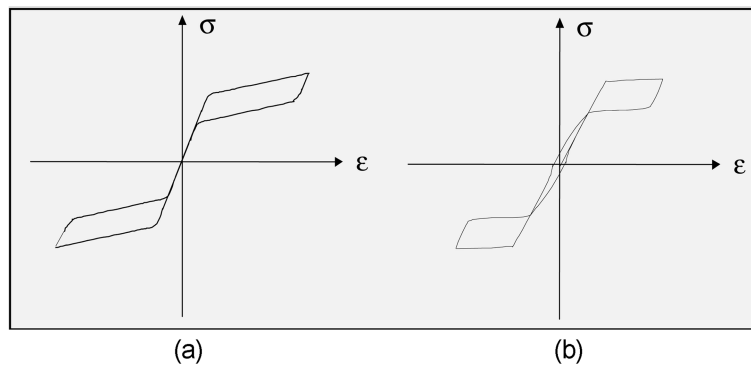


Fig. 3 σ - ε diagram: (a) small deformations $\varepsilon \sim 0.02$; (b) very small deformations $\varepsilon \sim 0.002$

where $\sigma_o > 0$ denotes the yielding stress (assumed to be equal in absolute value in traction $|\sigma_o'| = \sigma_o$ and in compression $|\sigma_o''| = \sigma_o$); therefore the modified version of the model is expressed by the relations

$$\begin{cases} \dot{\sigma} = E \left[\dot{\varepsilon} - \left| \dot{\varepsilon} \right| \left| \frac{\sigma - \beta}{\sigma_c} \right|^{d-1} \left(\frac{\sigma - \beta}{\sigma_c} \right) \right] \\ \beta = E \gamma \left\{ \left(\hat{\varepsilon} - \frac{\sigma}{E} \right) + \frac{2}{\pi} \psi |\varepsilon|^p \tan^{-1} [(\xi \varepsilon)^3 |\xi \varepsilon|^q] \right\} = E \gamma \left\{ \varepsilon_{in} + \frac{2}{\pi} \psi |\varepsilon|^p \tan^{-1} [(\xi \varepsilon)^3 |\xi \varepsilon|^q] \right\} \end{cases}$$

$$\text{with } \begin{cases} \gamma = \frac{\sigma_o - \sigma_c}{E \psi - \sigma_o} \\ \psi = c_\psi \frac{\sigma_o}{E} \\ \sigma_c = \nu \sigma_o \\ q < 1 \end{cases} \quad (13)$$

After selecting the reference mechanical model, one should suitably tune the SMA parameters in order to make the alloy to exhibit the super-elastic effect. Implementation of the mentioned stress-strain SMA relation in an ad-hoc compiled code would be, then, required for the treatment of pseudo-elasticity. Actually, in the specific case, rather than to the alloy itself one should directly refer to constitutive relations of the SMA tendons, as shown in the following step 2.

3.3.2. Step 2: specialising the general SMA model to the case of SMA tendons

In order to make the SMA devices to exhibit the pseudo-elastic behaviour, one is interested in specialising the previously given alloy stress-strain relation to the case of SMA tendons, where the normal forces $N_{io}^{(r)}$ (coinciding with $N_{io}^{+(r)}$ if $N_{io}^{+(r)} > 0$ or with $N_{io}^{-(r)}$ if $N_{io}^{-(r)} > 0$) and $N_{ie}^{(r)}$ (coinciding with $N_{ie}^{+(r)}$ if $N_{ie}^{+(r)} > 0$ or with $N_{ie}^{-(r)}$ if $N_{ie}^{-(r)} > 0$) in the currently stretched tendons at the i -th floor and their elongations $\Delta l_{io}^{(r)}$, $\Delta l_{ie}^{(r)}$ are to be related.

In order to allow some flexibility in the subsequent numerical investigation stage, thus introducing the possibility of freely varying the resistance of the SMA tendons at each floor, one initially refers to the generic SMA tendon with given resistance, and tunes all other parameters in order to make it to exhibit the super-elastic behaviour (as shown in the following step 3). Afterwards, when the parameters relevant to the tendon with prefixed resistance have been determined, the tendon model may be scaled by means of a factor, properly located in the formulas, in order to vary the strength of the tendon while keeping its super-elastic behaviour (in the numerical investigation the resistance of the tendons at each floor is proportioned, to some extent, to the floor resistance).

To this purpose, first of all one should go back to specialising Eq. (13) to the generic (currently stretched) SMA tendon with prefixed strength. Denoting by N its normal force and by Δl its elongation, the instantaneous rate relation (before time-discretization) is formally similar to that relevant to the alloy Eq. (13), i.e.

$$\left\{ \begin{array}{l} \dot{N} = k_s \left[\Delta \dot{l} - |\Delta \dot{l}| \left| \frac{N - \lambda}{N_c} \right|^{\bar{d}-1} \left(\frac{N - \lambda}{N_c} \right) \right] \\ \lambda = k_s \bar{\gamma} \left[\Delta \hat{l} - \frac{N}{k_s} + \frac{2}{\pi} \bar{\psi} |\Delta l|^{\bar{p}} \tan^{-1} [(\bar{\xi} \Delta l)^3 |\bar{\xi} \Delta l|^{\bar{q}}] \right] \end{array} \right\} \text{ with } \left\{ \begin{array}{l} \bar{\gamma} = \frac{N_o - N_c}{k_s \bar{\psi} - N_o} \\ \bar{\psi} = \bar{c}_\psi \frac{N_o}{k_s} \\ N_c = \bar{v} N_o \\ \bar{q} < 1 \end{array} \right. \quad (14)$$

where λ is the evolutionary one-dimensional *back-force*, N_c is the critical normal force given as a percentage \bar{v} of the yield normal force N_o (which represents the tendon resistance), k_s is the initial stiffness of the tendon and all other symbols denote tendon parameters.

3.3.3. Step 3: tuning the parameters of the SMA tendons

As emphasized at the previous step, after selecting the rate relations Eq. (14) of the generic (instantaneously stretched) SMA tendon (with prefixed resistance), one should suitably tune its parameters in order to get the super-elastic behaviour.

This purpose (i.e the treatment of pseudo-elasticity) requires the implementation of the rate relation Eq. (14) in an ad-hoc compiled code.

After the code is compiled, since most of the considered parameters jointly influence the basic characters of the constitutive relationships, it is necessary to determine the value of the parameters (able to make the tendon to show the pseudo-elastic behaviour) by trial and error.

Sample values of the SMA parameters resulting from this procedure (which takes a few minutes) are:

$$\begin{aligned} N_o &= 20,000 \text{ kg}, & k_s &= 140,000 \text{ kg} \cdot \text{cm}^{-1}, & \Delta \hat{l} &= 0 \text{ cm}, \\ \bar{d} &= 50, & \bar{p} &= 0.001, & \bar{c}_\psi &= 250, & \bar{v} &= 0.2, & \bar{\xi} &= 14, & \bar{q} &= 3/4. \end{aligned} \quad (15)$$

Once the tendon parameters have been selected for a given resistance, relations of the type Eq. (14) may be applied to each of the currently stretched tendons (after scaling at the desired tendon's resistance) at the i -th storey in order to instantaneously determine the tendons force contribution to the dynamic equilibrium of the floor. This last phase requires a further step 4 that involves the compilation of a subroutine devoted to the determination of the instantaneous SMA tendons force contributions on the basis of the knowledge of the instantaneous values of tendons elongations; the subroutine is to be suitably introduced in the general code that performs the time integration of the structure dynamic equilibrium equations.

3.3.4. Step 4: determining the instantaneous normal forces of the currently stretched SMA tendons

A subroutine implementing the SMA tendons relations (the basic parameters are now known after step 3 and only some scaling is required) is built up and introduced in the general code that simulates the structure response under dynamic excitation. The inputs of the subroutine are represented by the instantaneous elongations, rates of elongations and instantaneous forces of the currently stretched tendons at the i -th floor; the outputs are the instantaneous rates allowing to update the normal forces in

Table 2 Shear frame with SMA tendons: 25% SMA percentage

i th floor	PILES		TENDONS	
	u'_{oi}, u''_{oi} (cm)	T'_{oi}, T''_{oi} (kg)	$\Delta l'_{oi} \cos \alpha_i^+, \Delta l'_{oi} \cdot \cos \alpha_i^-$ (cm)	$N'_{oi} \cdot \cos \alpha_i^+, N'_{oi} \cdot \cos \alpha_i^-$ (kg)
1	±0.042673	±8534.700	±0.014224	±2844.900
2	±0.043767	±8128.286	±0.014589	±2709.429
3	±0.060059	±10295.83		
4	±0.062070	±9753.943		
5	±0.064484	±9212.058		
6	±0.067434	±8670.172		
7	±0.071122	±8128.286		

Table 3 Shear frame with SMA tendons: 50% SMA percentage

i th floor	PILES		TENDONS	
	u'_{oi}, u''_{oi} (cm)	T'_{oi}, T''_{oi} (kg)	$\Delta l'_{oi} \cos \alpha_i^+, \Delta l'_{oi} \cdot \cos \alpha_i^-$ (cm)	$N'_{oi} \cdot \cos \alpha_i^+, N'_{oi} \cdot \cos \alpha_i^-$ (kg)
1	±0.028449	±5689.800	±0.028449	±5689.800
2	±0.029178	±5418.857	±0.029178	±5418.857
3	±0.060059	±10295.83		
4	±0.062070	±9753.943		
5	±0.064484	±9212.058		
6	±0.067435	±8670.172		
7	±0.071122	±8128.286		

Table 4 Shear frame with SMA tendons: 75% SMA percentage

i th floor	PILES		TENDONS	
	u'_{oi}, u''_{oi} (cm)	T'_{oi}, T''_{oi} (kg)	$\Delta l'_{oi} \cos \alpha_i^+, \Delta l'_{oi} \cdot \cos \alpha_i^-$ (cm)	$N'_{oi} \cdot \cos \alpha_i^+, N'_{oi} \cdot \cos \alpha_i^-$ (kg)
1	±0.014224	±2844.900	±0.042673	±8534.700
2	±0.014589	±2709.429	±0.043767	±8128.286
3	±0.060059	±10295.83		
4	±0.062070	±9753.943		
5	±0.064484	±9212.058		
6	±0.067435	±8670.172		
7	±0.071122	±8128.286		

the tendons at the next step, i.e. the sought values $N_{io}^{(r+1)}$ (coinciding with $N_{io}^{+(r+1)}$ if $N_{io}^{+(r+1)} > 0$ or with $N_{io}^{-(r+1)}$ if $N_{io}^{-(r+1)} > 0$) and $N_{ie}^{(r+1)}$ (coinciding with $N_{ie}^{+(r+1)}$ if $N_{ie}^{+(r+1)} > 0$ or with $N_{ie}^{-(r+1)}$ if $N_{ie}^{-(r+1)} > 0$).

3.4. Numerical testing

For simulating the dynamic response of the frame equipped with SMA devices, one refers to the code based on the design details (relevant to the SMA tendons) reported in the previous Sect. 3.3; one considers a number of cases when the SMA tendons contribute to the total storey resistance by

absorbing a percentage of it equal to 25%, 50% and 75%.

In all of these cases, most of the dynamic excitation energy is dissipated by the SMA provision: under simply horizontal loads, the SMA members reduce the plastic phase in the structure’s response, attenuating the residual deformation of the structure, and, in the presence of P-Δ effects, they prevent the frame from reaching the failure condition.

As regards to the three mentioned cases of SMA tendons absorbing the 25%, 50% and 75% respectively of the total storey resistance, the mechanical characteristics of the entire system are given in Tables 2,3 and 4; here, with reference to the tendons, one reports the “equivalent” horizontal values of the involved quantities, i.e. of the limit values of elongation $\Delta l'_{oi}$ and of tensile normal force N'_{oi} in the reacting stretched tendon that end at the i -th floor (whose horizontal components are positive in the rightward direction and negative in the leftward direction).

Equivalent horizontal values of the quantities $\Delta l'_{oi}$ and N'_{oi} are obtained by multiplying each of them by $\cos\alpha_i^+$ and $\cos\alpha_i^-$, where the symbols $\alpha_i^+ = \alpha_{ie}^{+(1)}$, $\alpha_i^- = \alpha_{ie}^{-(1)}$ denote the two initial values (at time $t^{(r)} = 0$ and, thus, for $r = 1$) of the angles formed by the two tendons that end at the i -th floor with the floor itself.

In the numerical investigation one evaluates the quantities relevant to the maximum value of absolute inter-storey plastic drift $[\Delta u_p(t)]_{\max} = \max_{i=1,\dots,7} |\Delta u_{pi}(t)|$ in the structure; furthermore, since the response of the 1st and 2nd floor is the most significant (the upper part of the frame moves almost rigidly), the inter-storey drifts $\Delta u_1(t)$, $\Delta u_2(t)$ and the shear forces $T_1(t)$, $T_2(t)$ at the 1st and 2nd levels of the structure are monitored.

In Fig. 4 one can observe the comparison of the maximum absolute inter-storey plastic drift in the simple shear frame subject only to horizontal actions with the value attained in case of adopting SMA tendons for the three considered percentages. The same results are performed in Fig. 5 for the structure in the presence of vertical loads inducing P-Δ effects: one can notice that the beneficial effects of adopting SMA members are pretty evident since the failure condition is not reached anymore.

The hysteresis loops at the 1st and 2nd levels for the structure (without P-Δ effects) equipped or not

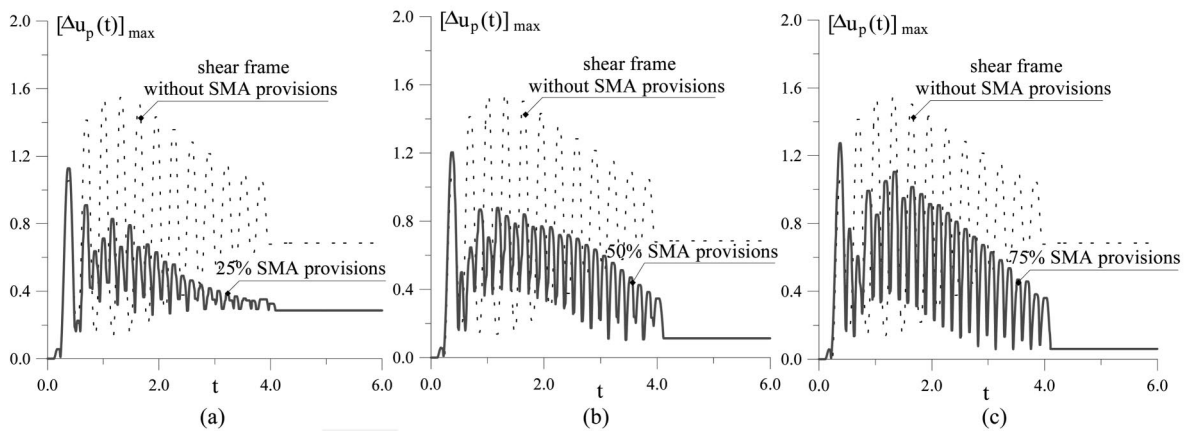


Fig. 4 Max plastic drift in the shear frame without P-Δ effect

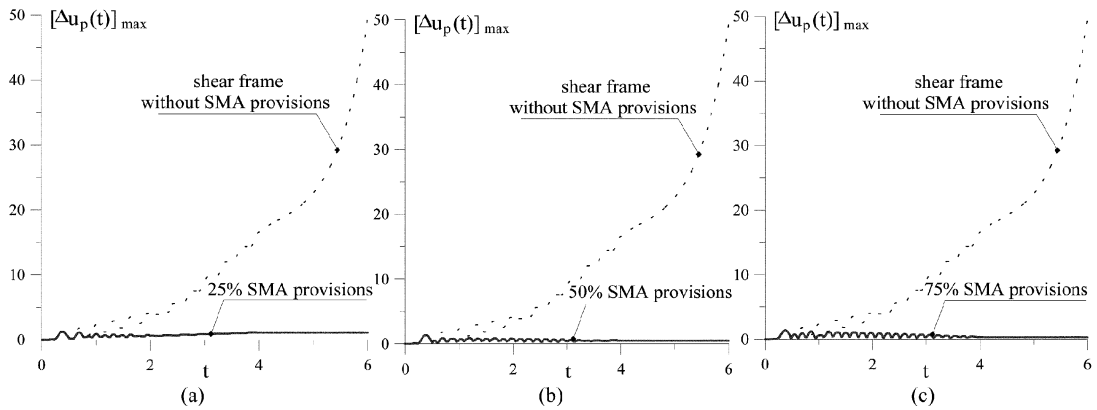


Fig. 5 Max plastic drift in the shear frame with P-Δ effect

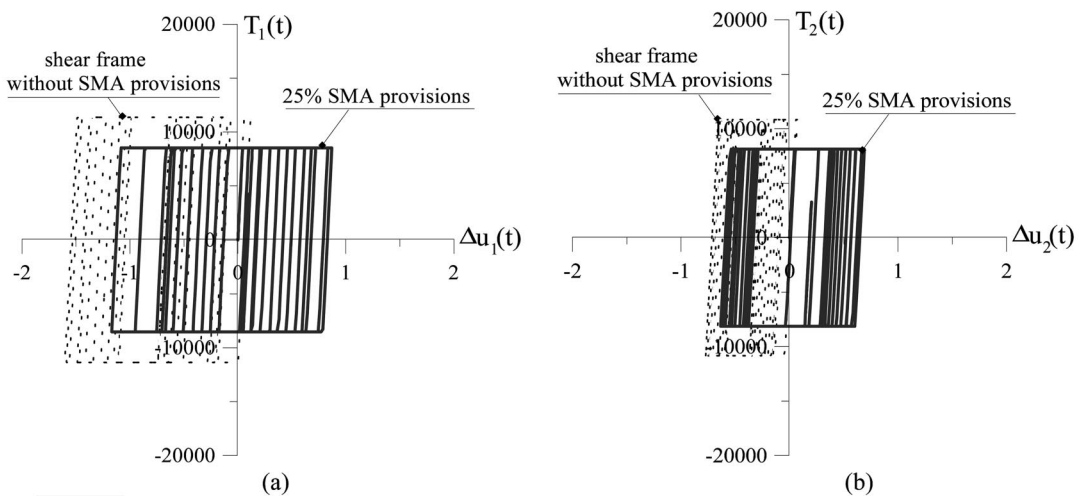


Fig. 6 No P-Δ effect: hysteresis loops at the 1st and 2nd floor in the shear frame with 25% SMA provisions

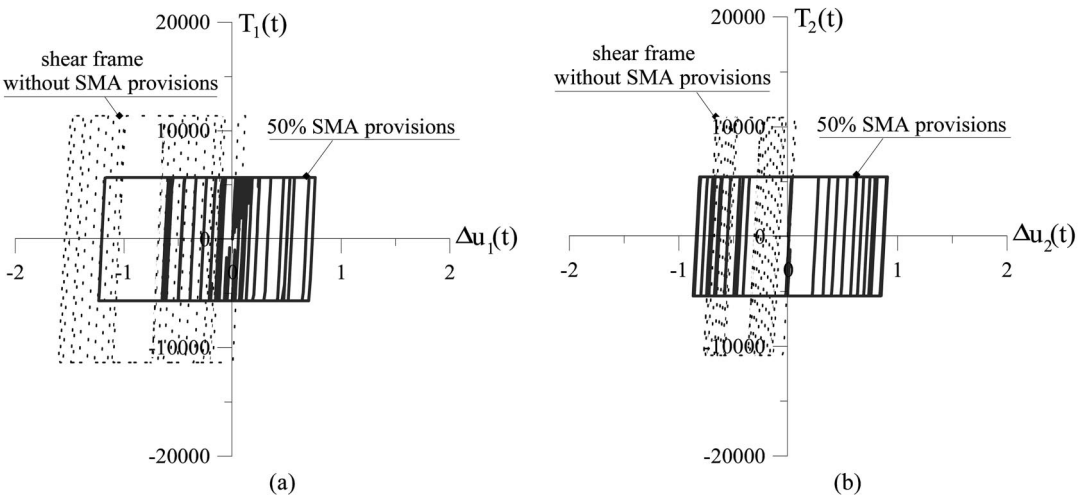


Fig. 7 No P-Δ effect: hysteresis loops at the 1st and 2nd floor in the shear frame with 50% SMA provisions

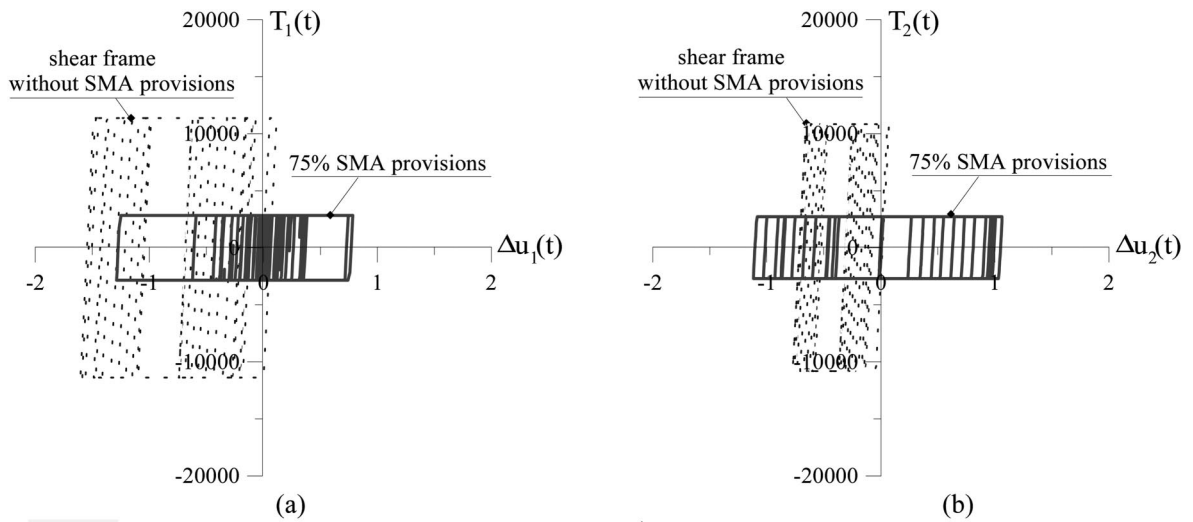


Fig. 8 No P-Δ effect: hysteresis loops at the 1st and 2nd floor in the shear frame with 75% SMA provisions

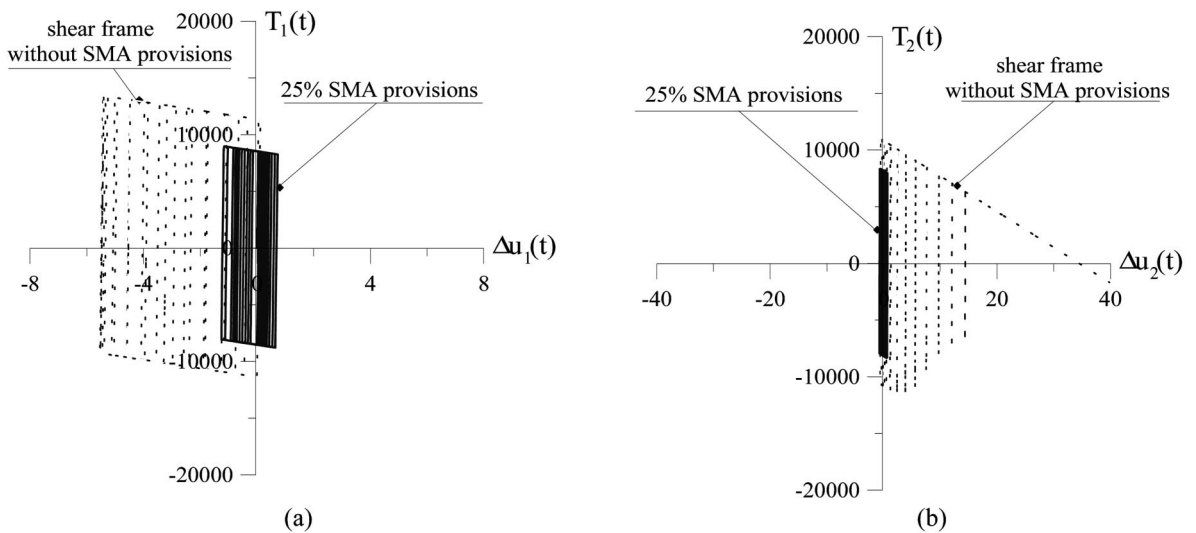


Fig. 9 P-Δ effect: hysteresis loops at the 1st and 2nd floor in the shear frame with 25% SMA provisions

with SMA provisions are reported in Figs 6, 7 and 8 for the 25%, 50% and 75% SMA percentage respectively. These results are reproduced in Figs 9,10 and 11 for the structure in the presence of P-Δ effects.

A wide response attenuation can be observed in case of adoption of SMA provision; one can particularly appreciate the high re-centring skill and low sensitivity to the P-Δ effects produced by SMA inclusions.

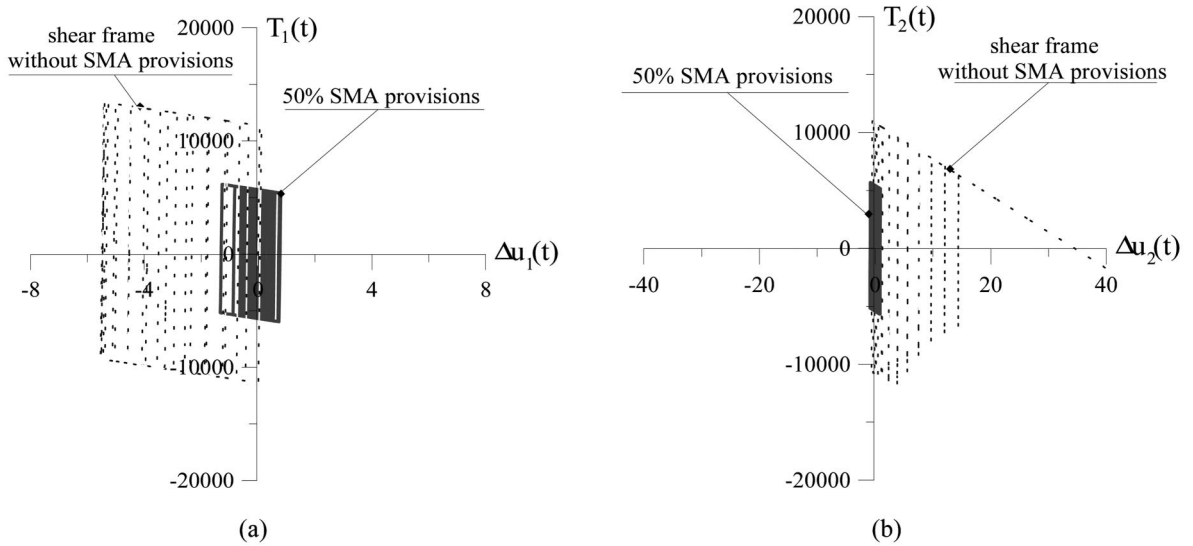


Fig. 10 P- Δ effect: hysteresis loops at the 1st and 2nd floor in the shear frame with 50% SMA provisions

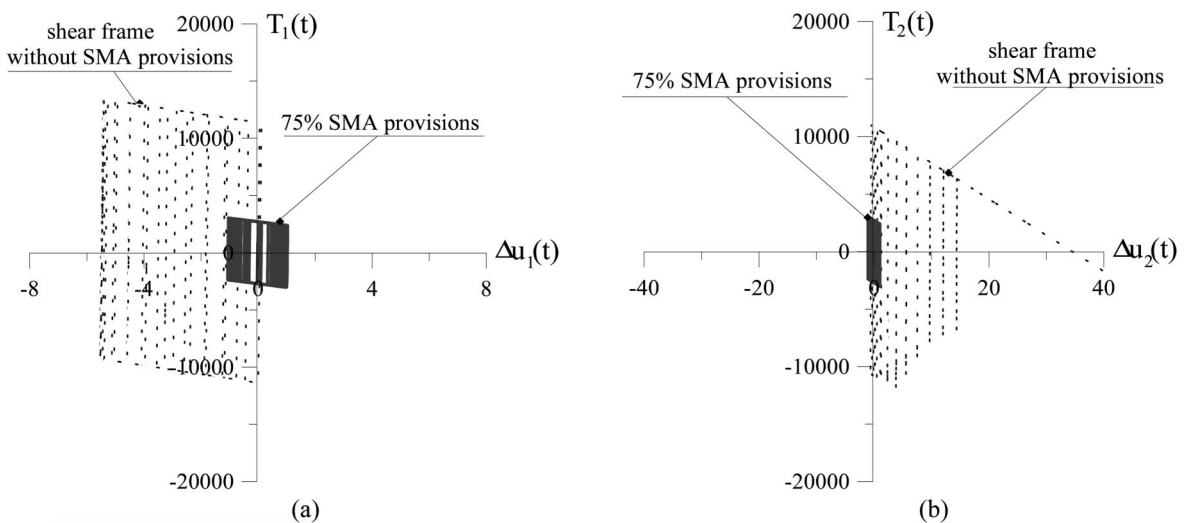


Fig. 11 P- Δ effect: hysteresis loops at the 1st and 2nd floor in the shear frame with 75% SMA provisions

As one can observe, the big advantage in increasing the SMA percentage of the contribution to the total storey resistance mainly lays in deeply bettering the re-centering capacity of the structure. Actually, even a small SMA percentage (25%) is able to significantly dissipate the incoming energy, but higher percentage values are required in order to obtain wide reduction of residual response values.

4. Conclusions

In the paper the convenience to provide ordinary structures with the inclusion of super-elastic resistant components has been tested and demonstrated, under the condition that the whole is properly designed. SMA members may be good candidates for this purpose, and a definite credit for such alloys can be assessed.

In details, the paper analyses the effects produced by SMA tendons contributing to the overall strength of a 7-storey elastic-plastic structural shear-frame undergoing horizontal shaking and subject to vertical loads. Special attention is devoted to attenuation of P- Δ effects. Pseudo-elastic SMA members are shown to decisively improve the dynamic response capacity of the structure either in terms of response reduction or of re-centering capacity.

The present results are the starting point to produce full models allowing for complete analysis, design and implementation of SMA applications in civil and seismic engineering, including all the complex phenomenology that is exhibited by these new materials.

Acknowledgements

Paper supported by grants of the Italian C.N.R. and co-financed by M.I.U.R.

References

- Armstrong, W.D. (1996), "A one-dimensional model of a shape memory alloy fiber reinforced aluminium metal matrix composite", *J. Intelligent Material Systems and Structures*, **7**, 448-454.
- Baratta, A., Corbi, O. (2003), "On the dynamic behaviour of elastic-plastic structures equipped with pseudoelastic SMA reinforcements", *J. Computational Materials Science*, Elsevier Science, **25**(1-2), 1-13.
- Baz, A., Iman, K., McCoy, J. (1990), "Active vibration control of flexible beams using shape memory actuators", *J. Sound and Vibration*, **140**, 437-456.
- Buehler, W., Wiley, R. (1965), "Nickel-based alloys", Technical Report, Naval Ordnance Lab.US-Patent 3174851.
- Corbi, O. (2001), "Analysis of dynamics of structures including S.M.A. members", *J. Structural Control*, Pitagora Ed., **8**(2), 189-202.
- Dolce, M., Cardone, D. and Marnetto, R. (2000), "Implementation and testing of passive control devices based on shape memory alloys", *J. Earthquake Engineering and Structural Dynamics*, **29**(7), 945-968.
- Duerig, T.W., Melton, K.N., Stolen, D. and Wayman, C.M. (Eds). (1990), *Engineering Aspects of Shape Memory Alloys*, Butterworth-Heinemann, London.
- Feng, Z.C., Li, D.Z. (1996), "Dynamics of a mechanical system with a shape memory alloy bar", *J. Intelligent Material Systems and Structures*, **7**, 399-410.
- Funakubo, K. (1984), *Shape Memory Alloy*, Gordon and Breach Science Publishers. New York.
- Graesser, E.J., Cozzarelli, F.A. (1991), "Shape memory alloys as new materials for aseismic isolation", *J. Engineering Mechanics*, ASCE, **117**, 2590-2608.
- Graesser, E.J., Cozzarelli, F.A. (1994), "A proposed three-dimensional constitutive model for shape memory alloys", *J. Intelligent Material Systems and Structures*, **5**, 78-89.
- Ikegami, R., Wilson, D.G., Anderson, J.R., Julien, G. (1990), "Active vibration control using NiTiNOL and piezoelectric ceramics", *J. Intelligent Materials and Structures*, **1**, 189-206.
- Liang, C. and Rogers, C.A. (1993), "Design of shape memory alloy springs with applications in vibration control", *J. Vibration and Acoustics*, **115**, 129-135.
- Liu, Y. and Van Humbeeck, J. (1999), "Damping capacity of shape memory alloy", *Proc. MANSIDE Project*, Final Workshop, Rome, Italy.
- Maclean, B.J., Patterson, G.J., Misra, M.S. (1991), "Modeling of a shape memory integrated actuator for vibration

- control of large space structures”, *J. Intelligent Material Systems and Structures*, **2**, 71-94.
- Müller, I. (1992), “Thermoelastic properties of shape memory alloys”, *Eur. J. Mechanics and Solids*, **11**, 173-184.
- Srinivasan, A.V. and McFarland, D.M. (2000), *Smart Structures*. Cambridge University Press, Cambridge, England.
- Thomson, P., Balas, G.J. and Leo, P.H. (1995), “The use of shape memory alloys for passive structural damping”, *J. Smart Materials Structures*, **4**, 36-42.
- Wayman, C.M., Duerig, T.W. (1990), “An introduction to martensite and shape memory in engineering aspects of shape memory alloys”, T.W. Duerig, K.N. Melton, D. Stolen and C.M. Wayman Eds: 3-20.
- Wayman, C.M. (1992), “Shape memory and related phenomena”, *J. Prog. Material Science*, **36**, 203-224.
- Wen, Y.K. (1976), “Method for random vibration of hysteretic systems”, *J. Engineering Mechanics Division*, ASCE, **102**(2), 249-263.

CC